International Journal of
MATERIALS RESEARCH

Zeitschrift für METALLKUNDE

Review



Lebiao Yang, Xiaona Ren, Changchun Ge, Qingzhi Yan

Institute of Powder Metallurgy and Advanced Ceramics, School of Materials and Engineering, University of Science and Technology Beijing, Beijing, P.R. China

# Status and development of powder metallurgy nickel-based disk superalloys

Nickel-based superalloys are crucial materials for the development of aero-engine components, since their excellent properties can meet the demands of turbine disks. For the formation of such alloys, powder metallurgy is considered as the ideal method, due to the resultant uniform composition and structure, fine grain, high yield strength, and good fatigue performance. This paper provides a critical review of the development of powder metallurgy nickel-based disk superalloys, their composition, as well as the evolution of the nickel-based superalloys' microstructure in the past few decades. Moreover, the influence of various elements on the material properties and the three major defects of powder metallurgy superalloys are reviewed. The analysis indicates that these defects may be directly or indirectly caused by the quality of the powder. Therefore, the innovative powder techniques of electrode induction melting gas atomization and spark plasma discharge spheroidization are presented, in order to prepare ceramic-free and superfine nickel-based superalloy powders. The powders prepared by electrode induction melting gas atomization and spark plasma discharge spheroidization have been found to be beneficial in improving the properties of powder metallurgy nickel-based disk superalloys.

**Keywords:** Nickel-based superalloys; Powder metallurgy; Turbine disks; Alloying elements; Defects

## 1. Introduction

Powder metallurgy (P/M) nickel-based superalloys are considered as a kind of back-bone materials in the aerospace field, since their performance is associated with excellent characteristics, such as high temperature strength, fatigue resistance, ductility, low creep, and structural stability [1–3]. In particular, owing to their promising properties, P/M nickel-based superalloys have been used in aero-engine hot section components, and account for approximately 50% of the weight of all components [4]. However, due to the fact that in the future the aero-engine thrust-weight ratio is expected to reach 15–20 [5], turbine disks will face much higher temperatures and pressures. Figure 1 shows the development trend of turbine inlet temperature, turbine disk temperature, and thrust-weight ratio of aero-engines [6].

In order to further improve the performance of P/M nickel-based superalloys, more requirements have been put forward for the composition design, powder preparation, and forming process of such superalloys. In this study, the development of P/M processes for nickel-based superalloys is reviewed. Moreover, two innovative superalloy powder technologies are introduced.

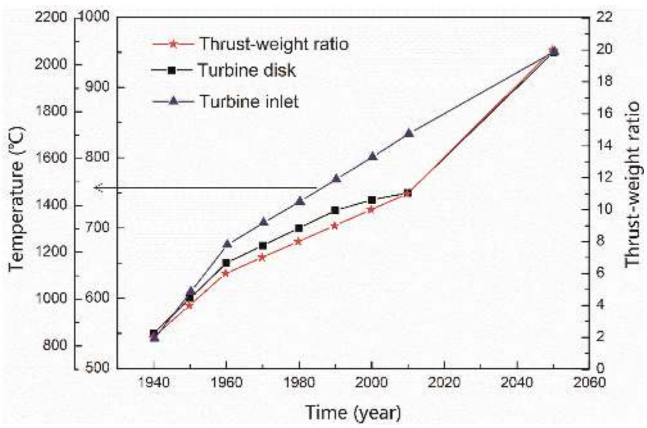


Fig. 1. Development trend of the turbine inlet temperature, turbine disk temperature, and thrust-weight ratio in aero-engine.

## 2. Development process of P/M superalloys

### 2.1. Development of P/M processes

The conventional casting process is suitable for producing superalloys with few elements, such as the Waspalloy which, along with Ni and Cr, contains only a small amount of strengthening elements (Al, Ti, and Nb). Unfortunately, the thermal properties of casting alloys can be deeply affected, since a large number of additional elements can cause segregation during the casting process. Besides, it is a common problem that cast alloys crack during hot-working processes [7–10]. Therefore, the P/M process has emerged.

In the P/M process, metal powder or mixtures with non-metal powders are used as raw materials [11]. In general, there are two types of production processes for disk superalloys [12]. The first is mostly used in the United States (Fig. 2), and consists of master alloy melting, argon atomization (AA), hot extrusion (HEX), and isothermal forging (ITF). The second process is preferred in Russia (Fig. 3), and consists of plasma rotating electrode processing (PREP) and hot isostatic pressing (HIP). Near net-shape HIPping is a new powder metallurgy processing technology which eliminates the extrusion and forging procedures and massive machining operations by using appropriate tooling for direct HIPping to produce near-shape or net-shape components. Moreover, near net-shape HIPing is expected to solve drawbacks, such as the long process time, high cost, and low fly-to-buy ratio [13–15].

### 2.2. Powder densification during the P/M process

It is generally considered that powder densification during P/M process can be divided into several stages [16–19] including mechanical compacts, plastic yield, creep, and diffusion. First of all, after the powder particles are packed into vessel prior to pressing and heating, point contact between particles takes place, which is called the particle rearrangement mechanism. Secondly, at the beginning of the heating and pressurizing stage, the powder particle state transforms from point contact to area contact, leading to elastic deformation. With increasing temperature and pressure, the deformation increases sharply, and as a result, necks will be formed between particles. In addition, at this stage, the particles undergo plastic deformation in a slipping manner. Thirdly, when the contact stress falls below the yield stress, densification will cease by plastic yielding. Plastic deformation does not occur during this period. Further densification depends mainly on law creep in the contact zones, which is the creep mechanism. In this stage, the density of the particles is close to the theoretical value. Next, due to some voids that are surrounded by spherical thick shells being retained [20], when densification occurs, material diffusion will take place through diffusion from the particle interior boundaries. Besides, since a concentration difference exists in particle interior and between particles, diffusion will also occur. Finally, the internal concentration tends to be balanced, the voids are filled, and the materials become denser.

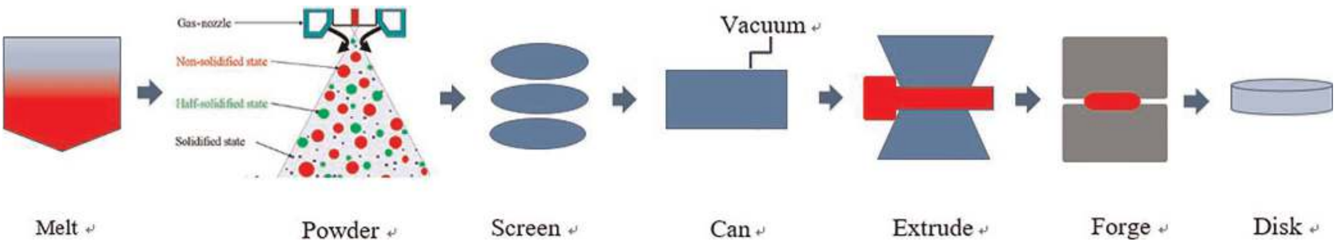


Fig. 2. Sequence of the conventional P/M process for powder disk superalloy.

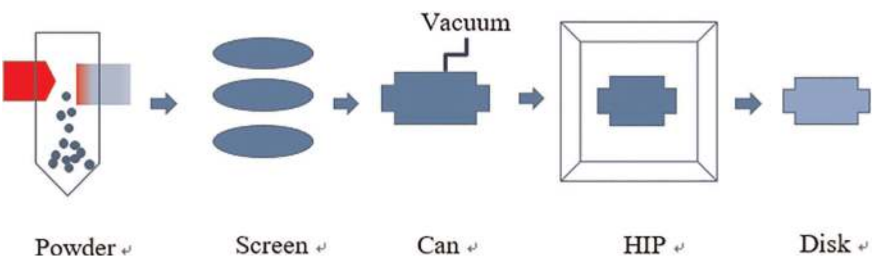


Fig. 3. Sequence of near net-shape HIPing for disk superalloy.

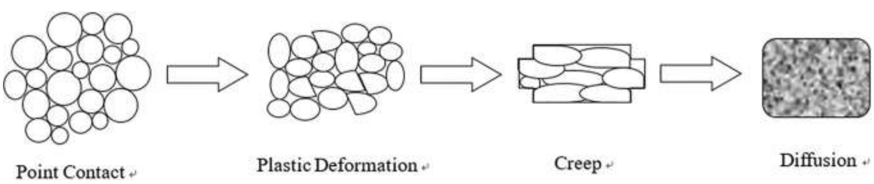


Fig. 4. The powder densification process.

Table 1. Composition and characteristics of P/M superalloys [12, 24–26].

| Genera-tion | Alloy | country | Compositions $\omega$(Ni-bal)(%) | | | | | | | | | | | | Physical parameters | | |
|---|---|---|---|---|---|---|---|---|---|---|---|---|---|---|---|---|---|
| | | | C | Co | Cr | w | Mo | Al | Ti | Nb | B | Zr | Hf | Other | $\omega(\gamma')$(%) | $T\gamma'$ (°C) | $P$ (g · cm$^{-3}$) |
| 1st | PA101 | USA | 0.15 | 9.00 | 12.50 | 4.00 | 2.00 | 3.50 | 4.00 | – | 0.015 | 0.10 | 1.00 | 4.00Ta | | | |
| | AF115 | USA | 0.05 | 15.00 | 10.50 | 6.00 | 2.80 | 3.80 | 3.90 | 1.8 | 0.02 | 0.05 | 0.80 | - | 55 | 1193 | 8.33 |
| | IN100 | USA | 0.08 | 18.50 | 12.50 | – | 3.40 | 5.50 | 4.50 | – | 0.02 | 0.05 | – | 0.75 V | 61 | 1185 | 7.90 |
| | Rene95 | USA | 0.06 | 8.00 | 13.00 | 3.50 | 3.50 | 3.50 | 2.50 | 3.5 | 0.01 | 0.05 | – | – | 50 | 1160 | 8.26 |
| | Astroloy | USA | 0.04 | 17.00 | 15.00 | – | 5.00 | 4.00 | 3.50 | – | 0.025 | 0.04 | – | – | 45 | 1145 | 8.02 |
| | LCAsto-loy | USA | 0.03 | 17.00 | 15.00 | – | 5.00 | 4.00 | 3.50 | – | 0.02 | 0.04 | – | – | 45 | 1145 | 8.00 |
| | MERL76 | USA | 0.02 | 18.50 | 12.40 | – | 3.20 | 5.50 | 4.30 | 1.40 | 0.02 | 0.06 | 0.40 | – | 64 | 1190 | 7.95 |
| | U720 | USA | 0.035 | 14.70 | 18.00 | 1.25 | 3.00 | 2.50 | 5.00 | – | 0.033 | 0.03 | – | – | 45 | 1150 | 8.10 |
| | API | UK | 0.03 | 17.00 | 15.00 | – | 5.00 | 4.00 | 3.50 | – | 0.025 | 0.04 | – | – | 50 | 1140 | – |
| | EP975P | RUS | 0.06 | 12.00 | 10.00 | 10.00 | 3.50 | 7.00 | 3.00 | 3.50 | – | – | 0.70 | – | 60 | 1230 | 8.47 |
| | EP741NP | RUS | 0.04 | 16.00 | 9.00 | 5.50 | 3.90 | 5.00 | 1.80 | 2.60 | 0.015 | 0.015 | 0.30 | 0.01Ge | 60 | 1180 | 8.35 |
| | FGH95 | CHN | 0.055 | 8.47 | 12.20 | 3.42 | 3.61 | 3.51 | 2.55 | 3.40 | – | – | – | – | 50 | 1160 | 8.27 |
| 2nd | Re-ne88DT | USA | 0.03 | 13.00 | 16.00 | 4.00 | 4.00 | 2.00 | 3.70 | 0.70 | 0.015 | 0.05 | – | – | 37 | 1135 | 8.26 |
| | U720Li | USA | 0.025 | 15.00 | 16.60 | 1.25 | 3.00 | 2.50 | 5.00 | – | 0.012 | 0.03 | – | – | 45 | 1150 | 8.10 |
| | N18 | FR | 0.02 | 15.50 | 11.50 | – | 6.50 | 4.30 | 4.30 | – | 0.015 | 0.03 | 0.50 | – | 55 | 1195 | 8.00 |
| | VV751P | RUS | 0.06 | 15.00 | 11.00 | 3.00 | 4.50 | 3.95 | 2.80 | 3.25 | 0.015 | – | 0.05 | 0.021La 0.01Mg | – | – | – |
| | FGH96 | CHN | 0.03 | 13.00 | 15.80 | 4.14 | 4.33 | 2.26 | 3.88 | 0.82 | – | – | – | – | 37 | 1135 | 8.32 |
| 3rd | Rene104 | USA | 0.04 | 20.00 | 13.10 | 1.90 | 3.80 | 3.70 | 3.50 | 1.20 | 0.03 | 0.05 | – | 2.30Ta | 51 | 1160 | 8.30 |
| | Allloy10 | USA | 0.04 | 15.00 | 11.00 | 5.70 | 2.50 | 3.80 | 1.80 | 1.80 | 0.03 | 0.10 | – | 0.90Ta | 55 | 1180 | – |
| | LSHR | USA | 0.03 | 21.30 | 12.90 | 4.30 | 2.70 | 3.40 | 3.60 | 1.40 | 0.03 | 0.05 | – | 1.70Ta | 60 | 1160 | – |
| | NF3 | USA | 0.03 | 18.00 | 10.50 | 3.00 | 2.90 | 3.60 | 3.60 | 2.00 | 0.03 | 0.05 | – | 2.50Ta | 55 | 1175 | – |
| | CH98 | USA | 0.05 | 17.90 | 11.60 | – | 2.90 | 3.90 | 4.00 | – | 0.03 | 0.05 | – | 2.90Ta | 58 | 1175 | – |
| | KM4 | USA | 0.03 | 18.30 | 12.00 | – | 4.00 | 3.80 | 4.90 | 1.90 | 0.03 | 0.04 | – | – | 56 | 1170 | – |
| | SR3 | USA | 0.03 | 11.90 | 12.80 | – | 5.10 | 2.60 | 4.90 | 0.015 | 0.03 | 0.03 | 0.20 | – | 49 | 1170 | – |
| | RR1000 | UK | 0.03 | 15.00 | 14.50 | – | 4.50 | 3.00 | 4.00 | – | 0.02 | 0.06 | 0.75 | 1.50Ta | 46 | 1160 | – |
| | N19 | FR | 0.015 | 12.20 | 13.30 | 3.00 | 4.60 | 2.90 | 3.60 | 1.50 | 0.01 | 0.05 | 0.25 | – | 43 | 1145 | 8.31 |
| | NR3 | FR | 0.02 | 14.90 | 12.50 | – | 3.55 | 3.60 | 5.50 | – | 0.01 | 0.03 | 0.30 | – | 53 | 1205 | 8.05 |
| | NR6 | FR | 0.02 | 15.30 | 13.90 | 3.70 | 2.20 | 2.90 | 4.60 | – | 0.01 | 0.03 | 0.30 | – | 45 | 1175 | 8.29 |

Notes: $\omega$ ($\gamma$')–Content of $\gamma$' (mass fraction),$T\gamma$'–Solution temperature of $\gamma$' (°C),$\rho$–density (g · cm$^{-3}$)

Actually, there is no clear critical point in these microscopic mechanisms during the densification process of superalloy powder particles. Sometimes these mechanisms interact and promote powder densification [21].

### 2.3. Development of P/M nickel-based superalloys

The origin of P/M nickel-based superalloys goes back in the 1960s [22] (Fig. 5). Until today, nickel-based superalloys have undergone three generations of development. The properties of nickel-based superalloys have also been greatly improved. It has been reported that in the United States, research on the fourth generation of P/M superalloys has already begun, in order to further improve the "three high and one low" performance of such superalloys (high temperature, high strength, high phase stability, and low fatigue crack growth rate) [23]. Superalloys prepared by P/M have the advantages of uniform composition and structure, and high fatigue and yield strength. Consequently, the P/M process is widely used to manufacture high performance aero-engine components.

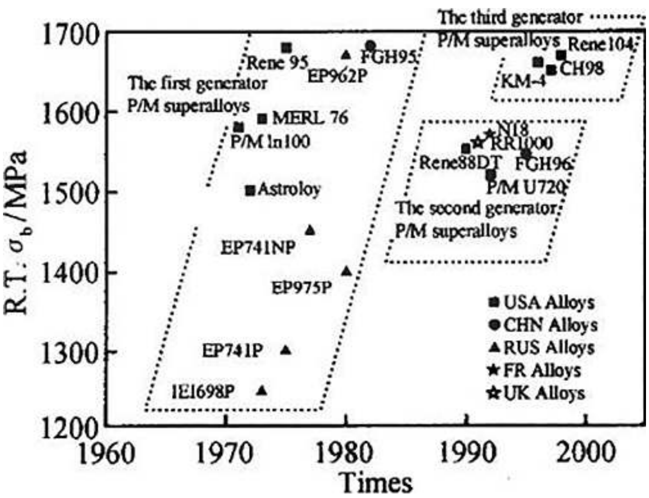


Fig. 5. Development timeline of nickel-based powder superalloys [22}.

As can be seen in Table 1 [12, 24–26], the content of Co has been slightly increased through the generations, and especially in the third generation. In the first and second generations of nickel-based superalloys, the content of Co ranges from 8 % to 18 %, while the content of Co reaches 21.3 % in third generation alloys such as LSHR. The content of Cr has been slightly decreased, but it remains between 9 % and 18 %. The content of precipitation strengthening elements Al, Ti, and Nb is between 6 % and 13.5 %. In addition, caution has been raised about the addition of grain boundary strengthening elements such as C, B, Zr, Hf and V.

### 2.4. Microstructural evolution

The evolution of the nickel-based superalloy microstructure during the past few decades is shown in Fig. 6 [27], which is magnified about 10000×. As is known, subsequently added elements create new microstructure, which promotes the improvement of alloy strength and ductility. At the same time, topological close-packed (TCP) phase forms, which is harmful to the superalloy material, since it increases its brittleness and decreases its strength [28–31]. As can be clearly seen in Fig. 6, from the early 1930s to 1950s, the development of alloys was mainly focused on "structure" increasing. In the first 20 years of development, the strengthening mechanism of nickel-based superalloys was mainly dependent on solid solution strengthening and carbide strengthening. After the 1950s, the main strengthening mechanism was solid solution strengthening and γ' phase strengthening. Nowadays, nickel-based superalloys have a high temperature capacity up to 850 °C, which is greatly improved compared to the initial stages.

## 3. Influencing factors on the P/M nickel-based disk superalloy properties

The research on nickel-based superalloys began in the 1930s, and was based on the Cr20Ni80 alloy. Due to their good strength, resistance to oxidation and corrosion resis-

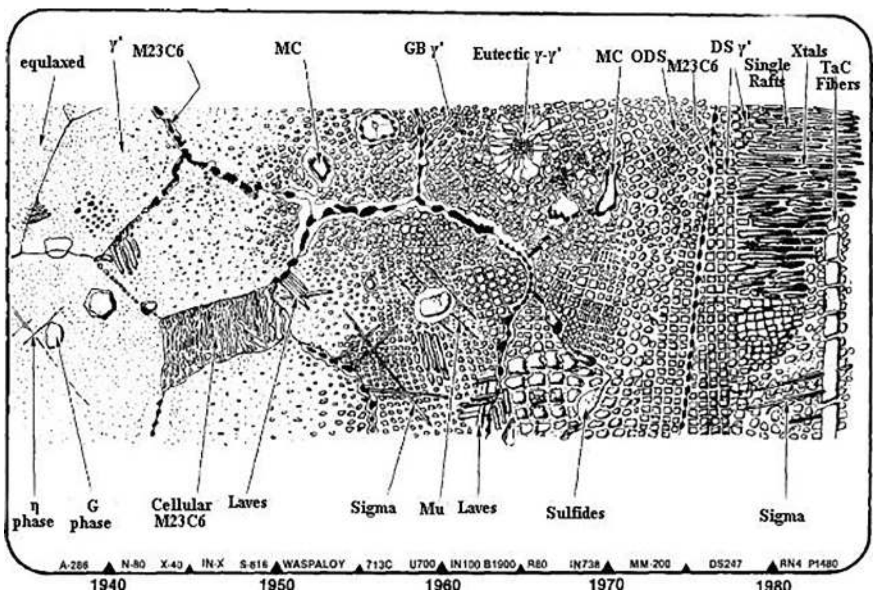


Fig. 6. Panorama of nickel-based superalloy microstructure development.

tance at high temperatures, they have been rapidly developed. The development of temperature bearing capacity of nickel-based superalloys is shown in Fig. 7 [32]. As can be seen the temperature bearing capability of the P/M nickel-based superalloys is higher than that of cast & wrought (C&W) superalloys. The P/M superalloy LSHR can withstand approximately 730 °C, which is significantly increased compared to early stage alloys. Due to the excellent overall performance at high temperatures and despite their defects, nickel-based superalloys have been widely used in many fields.

## 3.1. Influence of alloying elements

### 3.1.1. Role of various elements and topological dense phase formation

The quality of superalloys is not only related to the maturity of the P/M process, but also to the optimization of the superalloy composition. As compared to the initial stages, the composition of superalloys has become more and more complex. In order to meet application needs several new elements have been added to nickel-based superalloys. Different elements have different effects on the performance of superalloys. The effect of each added element on the performance of nickel-based superalloys can be seen in Fig. 8 [1]. Basically, the added elements affect the microstructure of the superalloy, which influences the overall performance. Some added elements cause solid solution atoms leading to lattice distortion, which will increase the dislocation movement resistance and make the plastic deformation more difficult [33, 34]. Therefore, the strength and hardness of the solid solution can be increased. In addition, the improvement of superalloy properties also relies on the precipitation of intermetallic compounds γ' ($Ni_3Al$, $Ni_3Ti$, etc.) and γ" ($Ni_3Nb$, $Ni_3V$, etc.), the uniform distribution of fine stable $M$C and $M_{23}C_6$ in crystal grains [35–39], and on elements such as B, Zr, and Re [40, 41], in order to purify and strengthen the grain boundaries. These additional elements are beneficial to the improvement of the superalloy performance, while at the same time can form harmful phases. For example, the added elements may result in alloy composition segregation. Additionally, excessive Cr, Nb, and Re may lead to precipitation of TCP phases, which will cause brittleness [42, 43]. Therefore, the content of additional elements should be controlled in a suitable range. For example, the content of carbon in a superalloy should be within 0.03–0.20 % [1].

## 3.2. Factors affecting material properties

As is well-known, the three major defects in P/M superalloy are prior particle boundary (PPB) precipitation, thermally induced porosity (TIP), and nonmetallic inclusions. These drawbacks have great influence on the performance of superalloy. Several studies have focused on reducing the effect of these defects on superalloys.

### 3.2.1. Prior particle boundary

One of the three major defects is superalloy-PPB precipitation along the prior particle boundaries, which consists of high-density carbide particles, oxide, oxy-carbides, and larger sized γ' phase [33, 44]. Much further and wider applications of superalloys are greatly restricted, since PPB has significant effects on their ductility, tensile strength, and high temperature creep behavior.

In general, many factors can lead to PPB precipitations. Some researchers believe that PPB formed due to powder surface contamination, since it can lead to increased oxygen and carbon content, and then the elements will segregate [45]. The carbides can be eliminated by high-temperature solution treatment, while, if the cooling rate is not correct, secondary precipitation will occur. Chang et al. developed a new method [46], called hot isostatic pressing, which in-

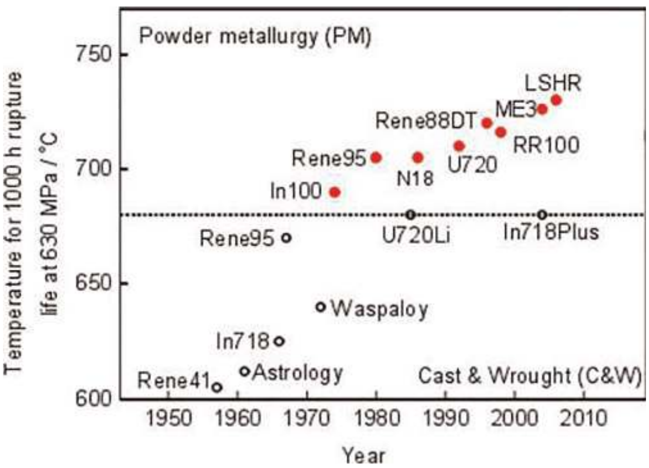


Fig. 7. Development of temperature bearing capability of Ni-based disk superalloy.

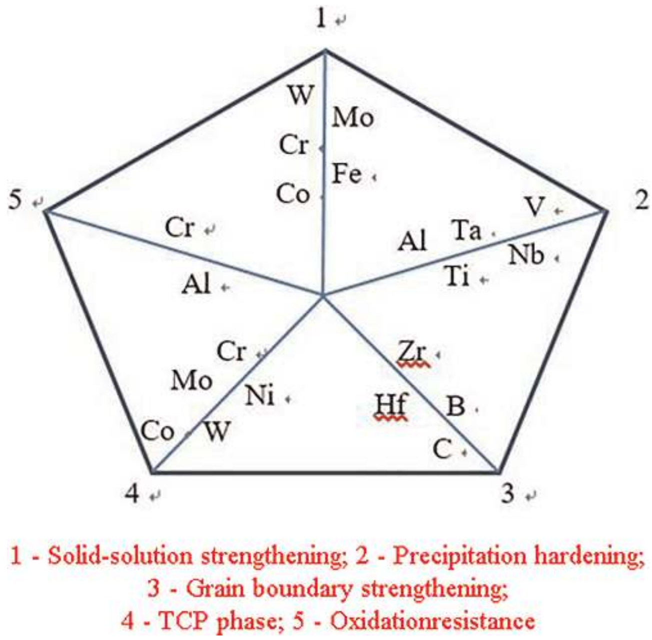


Fig. 8. Effects of different added elements on the properties of superalloys.

cludes a short holding time above the solidus temperature and a long annealing time below the incipient temperature of the Laves phase. It has been found that HIP can significantly reduce the PPBs and the Laves phase. In addition, several studies have investigated the influence of processing variables on PPB precipitation. It has been found that in P/M superalloy APKI, PPB precipitation can be suppressed under optimized HIP parameters [47].

#### 3.2.2. Thermally induced porosity

Thermally induced porosity (TIP) is caused by entrapped insoluble gases, which expand during post HIP thermal treatments and form discontinuous porosity in the product. It is widely accepted that the formation of TIP derives from the following reasons [48]: a) powder particles may actually be Ar bubbles, formed during Ar atomization; b) bubbles may exist if the powder is not sufficiently outgassed before pressurizing; c) the Ar pressing medium may be pumped into the product if there are leaks in the container. In addition, it is believed that the presence of TIP is detrimental to the mechanical properties of superalloy parts [49]. The effect of TIP on the tensile strength and yield strength of P/M superalloys has been studied by Zhang et al. [50], and their results revealed that the tensile strength will decrease with increasing porosity. Moreover, TIP can be a source of cracks after the post HIP process thermal treatment. It has been reported that an atomization technology can reduce TIP in $\gamma$' precipitation strengthened nickel-based superalloys [51].

#### 3.2.3. Inclusions

Many reports have shown that inclusions are harmful to the mechanical properties of superalloys, especially under low-cycle fatigue (LCF) [52–54]. The notched LCF behavior of P/M gas-turbine disks has been investigated [55], and the results indicated that the majority of LCF failures initiated from inclusions (oxides), with a minority of initiation sites being grain facets in the microstructure. The initiation sites are surface or subsurface, and reduced LCF life is generally associated with surface initiation at the notch root. In addition, crack nucleation around inclusions has a significant effect on the tensile strength of P/M superalloys [56]. In order to investigate the micro-crack nucleation mechanisms, electron backscatter diffraction (EBSD) combined with high spatial resolution digital image correlation (HR-DIC) were used [57], and the relative importance of inclusion/matrix shape on crack nucleation was found. The propagation mechanism of fatigue cracks initiated from inclusions has been examined in fine-grained IN718 [58]. On the basis that the faceted fatigue crack propagation time scales with the inclusion size, Denda. et al. found the significance of the inclusion size effect and developed a predictive protocol for determining this effect.

In general, the inclusions in P/M superalloy parts are mainly a result of two aspects [59–62]. a) they can be introduced during powder preparation processes. Despite processes such as screening and electrostatic separation being employed, the inclusions are difficult to completely remove. b) Inclusions can derive from the master alloy.

According to the aforementioned discussion, we can draw the conclusion that the mechanical properties of superalloys are highly related to the three major defects. Therefore, it is important to eliminate or reduce the effects of these defects. Moreover, it has been found that the raw powder quality may be associated with the formation of defects. Consequently, the preparation techniques of superalloy powders need to optimized.

## 4. Innovative technologies for nickel-based superalloy powders

High-quality superalloy powders guarantee the excellent performance of P/M nickel-based disk superalloys. As is known, there are several methods for producing metal powders [63]. Among them, inert gas atomization is mainly used for the preparation of superalloy powders. Currently, in the United States and some European countries the vacuum induction gas atomization process is mainly used to produce metal or alloy powders, while in Russia the plasma rotating electrode process (PREP) is adopted [63, 64]. In addition, in order to reduce the inclusions and refine the particle size of the powder as much as possible, new metal powder preparation methods have been proposed, such as the spark plasma discharge spheroidization process (SPDS) [65, 66] and electrode induction gas atomization (EIGA) [67, 68].

### 4.1. Spark plasma discharge spheroidization technique

#### 4.1.1. Mechanism of the spark plasma discharge spheroidization technique

The spark erosion technique was proposed by Svedberg in 1924 [69], and has been used to produce colloidal suspensions in the early years. Nowadays, it is widely used in applications in many industries, such as fabrication of hard or tough materials, wire-cutting, or powder production. American Materials and Electrochemical Research (MER) has used the plasma discharge spark process to produce ultrafine Ti and tool steel powders with tightly controlled size distribution ranging from 1 μm to 10 μm [70]. In addition, Ti–Ni–Zr and Ti–Ni–Hf powders have been obtained via spark-erosion in liquid argon from preliminary melted shape memory master alloys [71]. The Ge group was the first to report the preparation of superalloy powder using the spark erosion technique.

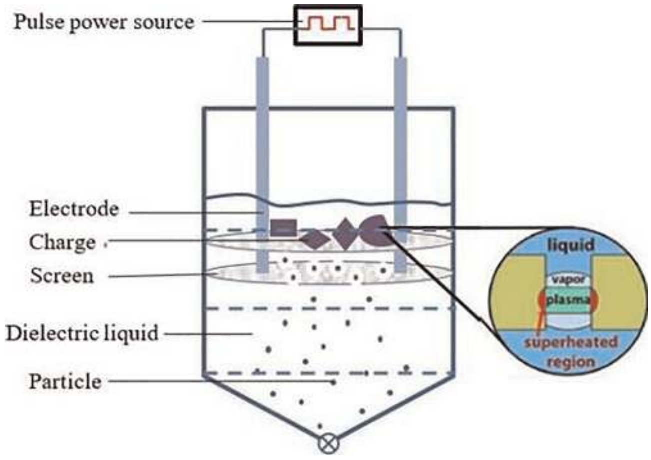


Fig. 9. Schematic diagram of SPDS.

The schematic diagram of spark erosion can be seen in Fig. 9 [72]. As can be seen, a repetitively pulsed spark discharge between the electrodes immersed in dielectric fluid is maintained. The forming mechanism of particles can be divided into four steps [73, 74]:

1. when the gap between the electrodes becomes narrow enough, a plasma channel is generated between the electrodes that are immersed in the dielectric fluid (water, kerosene, or liquid inert gas) and a pulsed power source, while the plasma channel is surrounded by a sheath of vaporized dielectric [75];
2. due to the repetitive spark discharge, a super-high temperature, as high as 10 000 K, develops at local of the electrode, which leads to localized melting or vaporization of the electrode;
3. the molten metal droplets and vapors are inserted into an insulating medium;
4. finally, the powders can be obtained by cooling of the molten droplets or condensation and cooling of the vapors in the dielectric liquid [76–78]. SPDS can avoid the introduction of ceramic during the powder preparation process.

#### 4.1.2. Superalloy powder prepared by SPDS

As can be seen in Fig. 10a, the resulted particle size is approximately $5 \sim 10$ μm, which means the powders produced by SPDS are fine. Due to the rapid cooling rate of $10^6 \sim 10^9$ $K \cdot s^{-1}$ [78], SPDS can produce ultrafine powders. Additionally, the cooling rate is faster than that in the argon atomization process ($10^3 \sim 10^5$ $K \cdot s^{-1}$). An SEM micrograph of Rene88DT superalloy particles produced by SPDS in alcohol and liquid argon is presented in Fig. 11a. It can be seen that the Rene88DT superalloy powder has a high degree of sphericity, smooth surface and uniform particle size [79]. A higher magnification SEM micrograph of the powder is displayed in Fig. 11b, and it can be seen that the surface of the powder particles exhibits cellular structures.

### 4.2. Electrode induction melting gas atomization (EIGA)

#### 4.2.1. Mechanism of the electrode induction melting gas atomization technique

The EIGA equipment was designed by the ALD company in order to solve the ceramic inclusions problem. It can be

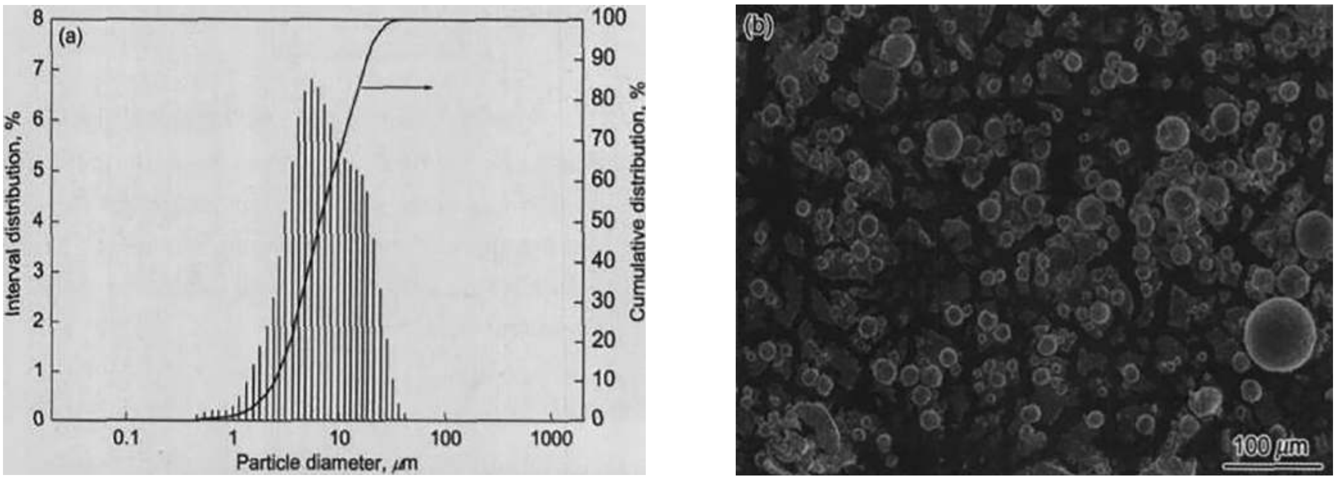


Fig. 10. (a) Particle size distribution, and (b) SEM micrograph of GH3039 powders prepared by SPDS.

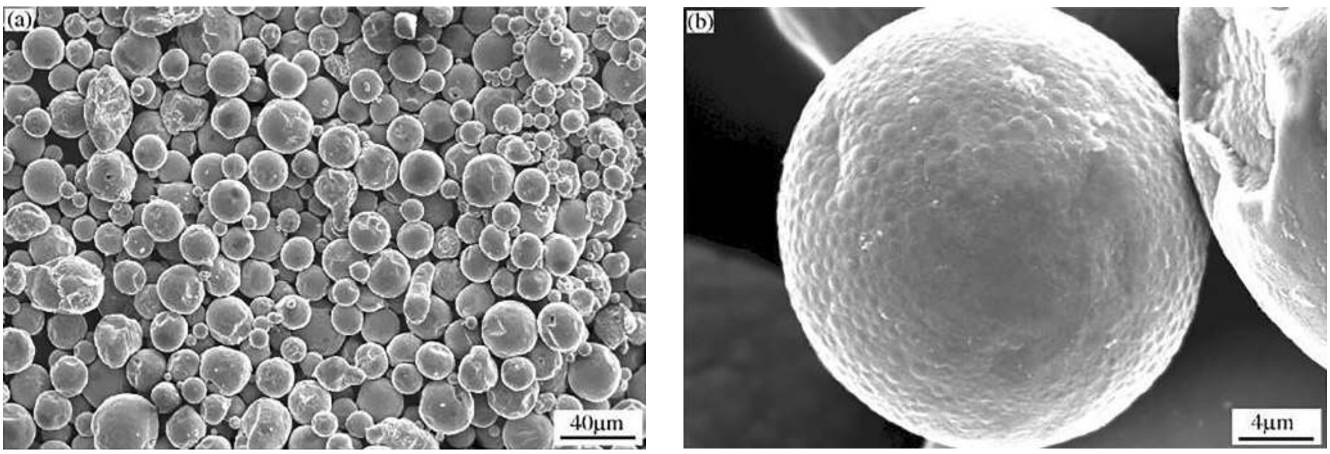


Fig. 11. SEM micrograph of Rene88DT superalloy powder produced by SPDS in alcohol and liquid argon: (a) low magnification; (b) high magnification [79].

seen from Fig. 12 that in this method a superalloy electrode is immersed in a conical induction coil and the molten metal falls directly into the atomization zone, and thus using a ceramic crucible can be avoided. Therefore, EIGA prevents the introduction of ceramics from the crucibles. The electrode bottom is immersed in an induction coil, where it melts and produces dripping or streaming liquid metal, which directly breaks down and is atomized by the high-pressure inert gas from the nozzles. Finally, the melt droplets cool and particles are obtained. In the past, EIGA was mainly used for the production of powders of Ti, Nb, Zr, and other low melting point alloys [80]. The Ge group was the first to propose the production of super-clean and super-spherical superalloy powders through EIGA by process parameter and nozzle optimization [68, 82].

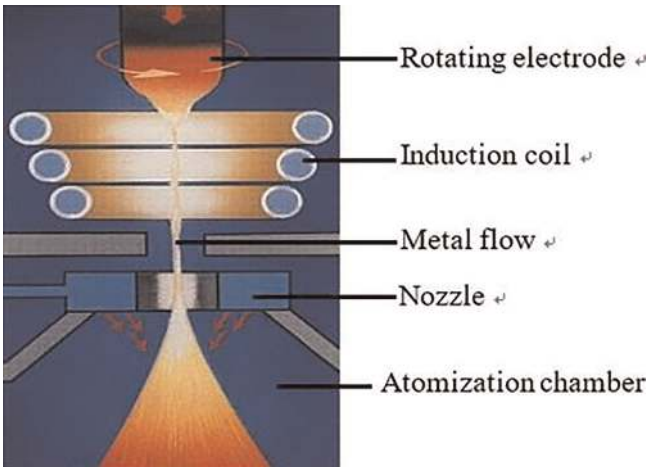


Fig. 12. Schematic diagram of the electrode induction melting gas atomization.

4.2.2. Superalloy powders prepared by EIGA

High-purity FGH4096 superalloy powder has been successfully prepared by EIGA. Figure 13a shows the distribution of particle diameter, which accounts for about 70 % in the range of 0 ~ 300 μm. As can be seen in Fig. 13b, the powder particles have high sphericity and smooth surface. The solidification microstructure of the particles ranging between 0 ~ 50 μm exhibits cellular structure. In particles whose size ranges between 50 ~ 100 μm, both cellular structure and dendritic microstructure occur. In particular, the dendritic microstructure increases rapidly when particle size is larger than 80 μm, and the cellular morphology will decrease at the same time. When the particle size is greater than 100 μm, the solidification microstructure of particles is dendritic. The reason why the surface solidification microstructure transforms from cellular to dendritic is probably a result of different cooling rates, since the fine particles cool faster than the coarse ones. In addition, there are no hollow particles ranging between 0 ~ 150 μm, while few hollow particles are present when the particle size is greater than 150 μm. This indicates that EIGA can effectively prevent TIP, which is caused by hollow particles [65].

4.2.3. Microstructure of nickel-based superalloy powders

The cross-sectional morphologies of nickel-based superalloy powders prepared by EIGA and SPDS are presented in Fig. 14. The internal structure of the powder prepared by EIGA is uniform (Fig. 14a), and dominated by dendritic structures, while on the other hand, the internal structure of the powder prepared by SPDS is uniform, small, with no obvious dendritic structures. One of the reasons explaining the different internal microstructures is supposed to be the different cooling rate. In addition, the cooling rate is also related to the particle size, since a higher cooling rate can produce smaller-sized powders. It has been reported that the cooling rate of gas atomization is approximately $10^3 \sim 10^5$ K · s$^{-1}$, while the cooling rate of SPDS is about $10^6 \sim 10^9$ K · s$^{-1}$. Therefore, the size of the powder particles prepared by SPDS is much smaller than of that prepared by EIGA.

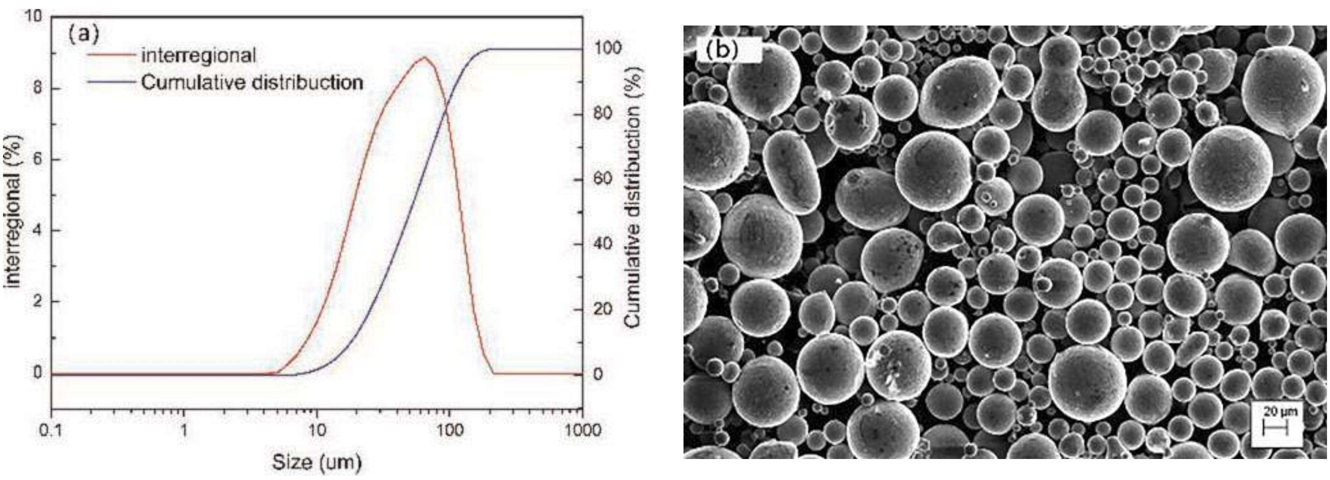


Fig. 13. FGH4096 superalloy powder produced by EIGA: (a) distribution of particle diameter, and (b) micro-topography.

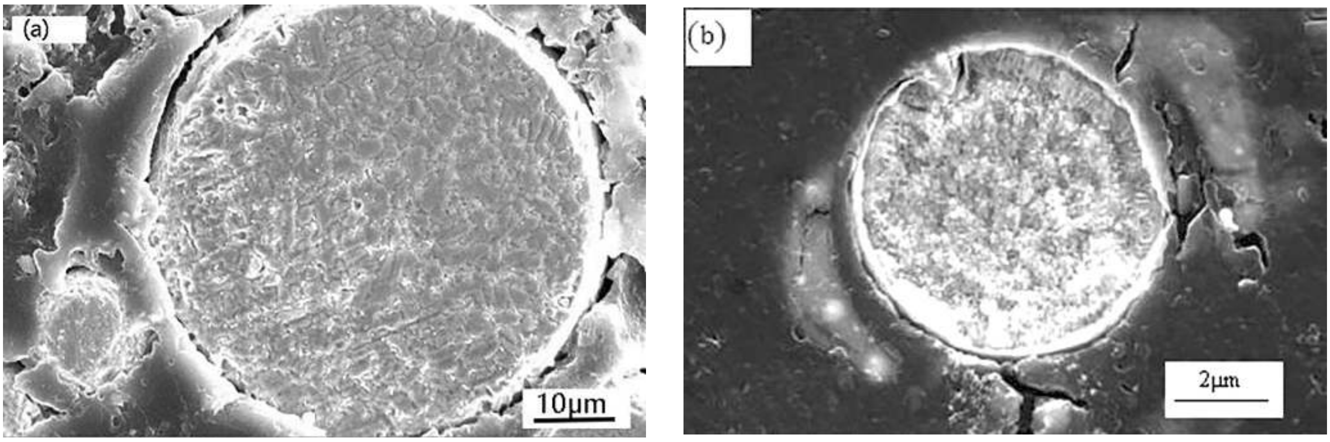


Fig. 14. Cross-section morphology of superalloy powders produced by (a) EIGA, and (b) SPDS.

## 5. Conclusions and outlook

P/M nickel-based superalloys are key materials for the production of high-temperature parts of aerospace engines. Thus, it is important to maintain and improve the high-temperature properties of nickel-based superalloys. According to the previously discussed studies, the following conclusions can be drawn:

1. The properties of nickel-based superalloys are influenced by their microstructure, and the role of various elements in superalloys has been well investigated. On this basis, composition optimization is a practical method for determining good combinations of mechanical properties of nickel-based superalloys. In addition, composition design of next generation high performance superalloys is also very important.
2. The powders prepared by SPDS have high degree of sphericity, smooth surface and uniform particle size ranging between $5 \sim 10$ μm. Thus, SPDS is an important supplement to the powder preparation techniques for P/M superalloys.
3. Powders prepared by EIGA have high sphericity, smooth surface, and few hollow particles. Inclusions derived from the crucible or tundish that contain the molten metal can be avoided by EIGA. Therefore, EIGA is beneficial to improve the performance of superalloys.

This work was supported by the Scientific Research Fund of Central Colleges and Universities(FRF-TP-17-044A1).

### References

[1] G.L. Chen: Superalloys. Metallurgical Industry Press. Beijing (1988).
[2] C.X Shi, Z. Zhong: Acta Metall. Sin. 33 (1997) 1. URL: http://www.ams.org.cn/EN/or http://www.ams.org.cn/EN/Y1997/V33/I1/1.
[3] R.C. Reed. The superalloys: fundamentals and applications. Cambridge: Cambrid- ge University Press. (2006) 217. PMid:17132965; DOI:10.1017/CBO9780511541285.006
[4] J. Li: Metal Mater. Res. 1 (2012) 5–5. DOI:10.1166/mat.2012.1022
[5] M. Sun, Z. Chang, Mo R. China Mech. Eng. 19 (2008) 200–203. 3–8984/20/42/425208. DOI:10.1088/095
[6] Y.F. Gu, C.Y. Cui, Y. Yuan, H.Z. Zhi: Acta Metall. 51 (2015) 1191. 0412.1961.2015.00442. DOI:10.11900/
[7] R. Chen: J. Mater. Eng. 18 (1998) 3.
[8] D.J. Brignell, K. Neailey: J. Mater. Prod. Technol. 138 (2003) 306./S0 924–0136 (03) 00090–6. DOI:10.1016
[9] G. Liu, L. Liu, G.J. Zhang, J. Zhang: Mater. Sci. Forum. 816 (2015) 608. www.scientific.net/MSF.816.608. DOI:10.4028/
[10] Y. Liu, R. Hu, J.S. Li, H.C. Kou, H.W. Li, H. Chang, H.Z. Fu: Mater. Sci. Eng. A 508 (2009) 141. DOI:10.1016/j.msea.2008.12.032
[11] P.Y. Huang: Powder metallurgy principle. Metallurgical Industry Press. Beijing (1982).
[12] Y.W. Zhang, J.T. Liu: Mater. China (2013) 1.
[13] J.H. Moll, J.J. Conway: Superalloys. (2000) 135. oys_2000_135_142. DOI:10.7449/2000/Superall-
[14] R. Baccino, F. Moret, F. Fellerin, D. Guichard, G. Raisson: Mater. Des. 21 (2000) 345. DOI:10.1016/S0261-3069(99)00093-X
[15] C. Broeckmann: Powder Metall. 55 (2013) :176. 000000063. DOI:10.1179/0032589912Z.00
[16] W. Voice, M. Hardy, D. Rugg: Powder Metallurgy World Congress & Exhibition (PM2004) (2004) 6. (05) 00388–7. DOI:10.1016/S0026-0657
[17] E. Arzt, M.F. Ashby, K.E. Easterling: Metall. Trans. A 14 (1983) 211. 7/BF02651618. DOI:10.100
[18] F.B. Swinkels, D.S. Wilkinson, E. Arzt, M.F. Ashby: Acta Metall. 31 (1983) 1829. (83) 90129–3. DOI:10.1016/0001-6160
[19] J Besson, F Valin, P Lointier, M Boncoeur: J. Mat. Eng. Perform. 1 (1992) 637. DOI:10.1007/BF02649245
[20] C.L. Qiu: PhD thesis, Net-shape hot isostatic pressing of a nickel-based powder superalloy, University of Birmingham (2010).
[21] F.K. Ma: Isostatic technology. Metallurgical Industry Press. Beijing. (1992).
[22] J.W. Zhou, W.X. Wang: J. Aeronaut. Mater. 26 (2006) 000244./j.issn.1005–5053. 2006.03.051. DOI:10.3969
[23] G.Q. Zhang: Adv. Mater. Ind. (2009) 11. 2009. 11.004. DOI:10.3969/j.issn.1008-892X
[24] Z. Ying: J. Iron Steel Res. 12 (2000) 63–69.
[25] S.F. Tian, GQ. Zhang, Z. Li, MG. Yan: J. Aeronaut. Mater. (2003) z1. 2003.z1.052. DOI:10.3969/j.issn.1005-5053
[26] W. Cai, E.J. Lavernia. Metall. Mater. Trans. B 29 (1998) 1097–1106. DOI:10.1007/s11663-998-0079-x
[27] C.T. Sims: Superalloys. (1984) 399. 9_419. DOI:10.7449/1984/Superalloys_1984_39
[28] J. Ye: American nickel-based superalloy. Science Press. Beijing (1978).
[29] M.C. Hardy, B. Zirbel, G. Shen, R. Shankar: Superalloys. (2004) 83. 49/2004/Superalloys_2004_83_90. DOI:10.74
[30] G.B. Olson, H.J. Jou, J. Jung, J.T. Sebastian, A. Misra, I. Locci, & D Hull: Superalloys. (2008). DOI:10.7449/2004/Superalloys_2004_83_90
[31] J.H. Zhuab, L.M. Pikea, C.T. Liua, P.K. Liawb: Acta Mater. 47 (1999) 2003. DO I:10.1016/S1359–6454 (99) 00090–7. DOI:10.1016/S1359-6454(99)00090-7
[32] Y.F. Gu, C. Cui, H. Harada, T. Fukuda, D. Ping, Mitsuhashi, A., Fujioka, J: Superalloys (2008) 53. DOI:10.7449/2008/Superalloys_2008_53_61
[33] W. Yang, J. Mao, W. Wang, J. Zou, R. Zhou: J. Univ. Sci. Technol. Beijing (1987) (s1) 90.

[34] B.F. Hu, G.F. Tian, C.C. Jia, G.Q. Liu: J. Aeronaut. Mater. 27 (2007) 80. DOI:10.3969/j.issn.1005-5053.2007.04.017
[35] Y.W. Zhang, F.M. Wang, B.F. Hu: Acta Metall. Sin. 48 (2012) 1011./SP.J.1037.2012.00136. DOI:10.3724
[36] B.F. Hu, G.Q. Liu, K. Wu, P.H. Hu: Acta Metall. Sin. 48 (2012) 830. DOI:10.3724/SP.J.1037.2012.00226
[37] S. Ochial, Y. Oya, T. Suzuki: Acta Metall. 32 (1984) 289. (84)90057–9. DOI:10.1016/0001-6160
[38] H. Sugimura, Y. Kaneno, T. Takasugi: Mater. Sci. Forum 654 (2010) 440. DOI:10.4028/www.scientific.net/MSF.654-656.440
[39] X.Z. Qin, J.T. Guo, C. Yuan, C.L. Chen, J.S. Hou, H.Q. Ye: Mater. Sci. Eng. A 485 (1–2) (2008) 74. DOI:10.1016/j.msea.2007.07.055
[40] K. Wu, G.Q. Liu, B.F. Hu, H. Wu, Y.W. Zhang: J. Univ. Sci. Technol. Beijing, 32 (2010) 1464. (10) 60661–9. DOI:10.1016/S1003-6326
[41] T.J. Garosshen, T.D. Tillman, G.P. Mccarthy: Metall. Trans. A 18 (1987) 69. DOI:10.1007/BF02646223
[42] J.X. Yang, Q. Zheng, X.F. Sun, H.R. Guan, Z.Q. Hu: Mater. Sci. Eng. A 465 (2007) 100. 1016/j.msea.2007.01.152. DOI:10
[43] K. Matuszewski, R. Rettig, H. Matysiak, Z. Peng, I. Povstugar, P. Choi, J. Müller, D. Raabe, E. Spiecker, K.J. Kurzydłowski, R.F. Singer: Acta Mater. 95 (2015) 274. DOI:10.1016/j.actamat.2015.05.033
[44] E. Ott, T. Gabb, R. Helmink, A. Wusatowska-Sarnek, in: 8th Int. Symp. Superalloy 718 and Derivatives, John Wiley & Sons, Inc.: Hoboken, NJ, USA (2014) 447–458. DOI:10.1002/9781119016854.ch35
[45] G.A. Rao, M. Srinivas, D.S. Sarma: Mater. Sci. Eng. A 383 (2004) 201. 1016/j. msea. 2004.05.062. DOI:10
[46] L. Chang, W. Sun, Y. Cui, R. Yang: Mater. Sci. Eng. A (2016) 682. DOI:10.1016/j.msea.2016.11.031
[47] R. Thamburaj, W. Wallace, Y.N. Chari, T.L. Prakash. Powder Metall. 27 (1984) 169. DOI:10.1179/pom.1984.27.3.169
[48] R.L. Dreshfield, R.V. Miner: Powder Metall. Int. 31 (1980) 102 02655199. DOI:10.1007/bf
[49] G. He, F. Liu, L. Huang, L. Jiang: Adv. Eng. Mater. 18 (2016) 1823. DOI:10.1002/adem.201600270
[50] G.X. Zhang, S.B. Han, Z.K. Sun: Powder Metall. Ind. (2015).
[51] E.S. Huron. Method for reducing thermally induced porosity in a polycrystalline nickel-base superalloy article: US Patent: us5584948 (1996).
[52] E.S. Huron, P.G. Roth: Superalloys. (1996) 359. Superalloys_1996_359_ 368. DOI:10.7449/1996/
[53] Y. Zhang, Y. Zhang, P. Song, F. Zhang, Y. Tao: J. Iron Steel Res.(2003).
[54] J.C. Stinville, V.M. Miller, T.M. Pollock: Superalloys 2016. Proceedings of the 13th Intenational Symposium of Superalloys. (2016). ch96. DOI:10.1002/9781119075646
[55] A.M. Wusatowska-Sarnek, P. Bhowal, D. Gynther, Mater. Sci. Forum. Trans Tech Publications, 539 (2007) 2960–2965. MSF.539–543. 2960. DOI:10.4028/www.scientific.net/
[56] J. Jiang, J. Yang, T. Zhang, J. Zou, Y. Wang, F.P.E. Dunne, T.B. Britton: Acta Mater. 117 (2016) 333. DOI:10.1016/j.actamat.2016.07.023
[57] J. Jiang, J. Yang, T.T. Zhang, P.E. Dunne, T. Ben Britton: Acta Mater. 97 (2015) 367. DOI:10.1016/j.actamat.2015.06.035
[58] T. Denda, P.L. Bretz, J.K. Tien: Metall. Trans. A 23 (1992) 519. BF02801169. DOI:10.1007/
[59] G. Miao, X. Yang, D. Shi: Mater. Sci. Eng. A 668 (2016) 66–72. msea.2016. 05. 034. DOI:10.1016/j
[60] S.Q. Cheng, B.Y. Huang: Powder Metall. Technol. 5 (2004) 009. 108819802766269511. DOI:10.1162/
[61] D.R. Chang, D.D. Krueger, R.A. Sprague: Superalloys 1984. Proceedings of the Fifth International Symposium on Superalloys. (1984) 245. Superalloys_1984 _245_273. DOI:10.7449/1984/
[62] W. Guo: Mater. Rev. 18 (2004) 87. DOI:10.1109/JLT.2003.821766
[63] G.H. Gessinger, M.J. Bomford: Powder Metallurgy of Superalloys. Butterworths. (1984). DOI:10.1179/imtlr.1974.19.1.51
[64] Z. Han, G. Zeng, S. Liang, X. Chen, P. Zhang: Mater. China 2014. issn.1674–3962.2014.12.05. DOI:10.7502/j
[65] C.L. Jia, C.C. Ge, Q.Z. Yan: Chin. Phys. B 25 (2016) 320. -1056/ 25/2/026103. DOI:10.1088/1674
[66] C.C. Ge, C.L. Jia, Q.Z. Yan: National Powder Metallurgy Conference. (2015). DOI:10.1088/1674-1056/25/2/026103
[67] M. Hohmann, S. Pleier: Acta Metall. Sin. (English Letters) 18 (2005) 15. 1016/j.msea.2005.02.012. DOI:10
[68] R. Gerling, M. Hohmann, F.P. Schimansky: Mater. Sci. Forum. 539 (2007) 2693. DOI:10.4028/www.scientific.net/MSF.539-543.2693
[69] T. Svedberg, C. Chemisty: The chemical catalog company. New York. (1924).
[70] K. Newell: Metal Powder Report. 54 (1999) 22. 0657 (99) 80499–8. DOI:10.1016/S0026-
[71] G. Monastyrsky, P. Ochin, G.Y. Wang, V. Kolomytsev, Y. Koval, A. Gilchuk, S. Zaharchenko: 4 (2011) 188. www.chemetal-journal.org.
[72] P.K. Nguyen, K.H. Lee, J. Moon, S.I. Kim, K.A. Ahn, L.H. Chen, S.M. Lee, R.K. Chen, S. Jin, A.E. Berkowitz: Nanotechnology. 23 (2012) 415604. -4484/23/41/415604. DOI:10.1088/0957
[73] C.C. Ge, J. Yu, W.P. Shen: Mater. Sci. Forum. 561 (2007) 861–863. DOI:10.4028/www.scientific.net/MSF.561-565.861
[74] X.J. Hai: MSc thesis, Beijing University of Science and Technology. (2015).
[75] A.E. Berkowitz, M.F. Hansen, F.T. Parker, K.S. Vecchio, F.E. Spada, E.J. Lavernia, R. Rodriguez: J. Magn. Magn. Mater. 254 (2003) 1. S0304–8853(02)00932–0. DOI:10.1016/
[76] M.S. Hsu, M. Meyers, A.E. Berkowitz: Scr. Metall. Mater. 32 (1995) 805. DOI:10.1016/0956-716X(95)93205-I
[77] C.C. Ge; J. YU: Acta Metall. Sin. 44 (2008) 892. 412–1961. 2008.07.024. DOI:10.3321/j.issn:0
[78] A.E. Berkowitz, J.L. Walter: J. Mater. Res. 2 (1987) 277. 7. 0277. DOI:10.1557/JMR.198
[79] J.M. Bao, C.C. GE, S.Q. Guo, Y. Zhang, W.P. Shen. Powder Metall. Ind. (2010).
[80] L.K W, R. Gerling, F.P. Schimansky: Scr. Mater. 42 (1999) 601. 6/S1359–6462(98)00493-X. DOI:10.101
[81] W. G, R. Gerling, F.P. Schimansky: Acta Mater. 51 (2003) 741–752. 1016/S1359–6454(02)00465–2. DOI:10
[82] S. Feng, M. Xia, C.C. Ge: Chin. Phys. B 27 (2018) 044701. -1056/ 27/4/044701. DOI:10.1088/1674

(Received August 23, 2018; accepted April 2, 2019; online since September 2, 2019)

**Correspondence address**

Xiao-Na Ren
Institute of Powder Metallurgy and Advanced ceramics,
School of Materials and Engineering
University of Science and Technology Beijing
Xueyuan Road 30#
Beijing 100083
P.R. China
E-mail:renxn@ustb.edu.com

Chang-Chun Ge
Institute of Powder Metallurgy and Advanced ceramics,
School of Materials and Engineering
University of Science and Technology Beijing
Xueyuan Road 30#
Beijing 100083
P.R. China
E-mail: ccge@mater.ustb.edu.cn
Tel: +86 10-62334951
Fax: +86 10-62334951
E-mail: ccge@mater.ustb.edu.cn

**Bibliography**
DOI 10.3139/146.111820
Int. J. Mater. Res. (formerly Z. Metallkd.)
110 (2019) 10; page 901–910

ISSN 1862-5282